



## Cause of the widening of the tropical belt since 1958

Jian Lu,<sup>1,2,3</sup> Clara Deser,<sup>1</sup> and Thomas Reichler<sup>4</sup>

Received 22 September 2008; revised 9 December 2008; accepted 30 December 2008; published 5 February 2009.

[1] Previous studies have shown that the width of the tropical belt has been increasing since at least the late 1970s based on a variety of metrics. One such metric, the frequency of occurrence of a high-altitude tropopause characteristic of the tropics, is used here to show that the observed widening of the tropics can be accurately replicated by an atmospheric general circulation model forced by the observed evolution of global SST and sea ice distributions as well as the direct radiative effects from both natural and anthropogenic sources. Contrasting this simulation with one forced by the observed SST and sea ice distributions alone reveals that the widening trend can be attributed entirely to direct radiative forcing, in particular those related to greenhouse gases and stratospheric ozone depletion. SST forcing causes no significant change in the width of the tropics, and even a contraction in some seasons. **Citation:** Lu, J., C. Deser, and T. Reichler (2009), Cause of the widening of the tropical belt since 1958, *Geophys. Res. Lett.*, 36, L03803, doi:10.1029/2008GL036076.

### 1. Introduction

[2] There is growing evidence from a variety of data sources that the tropics have been widening, at least since the beginning of the satellite era (1979). For example, *Hudson et al.* [2007] used the gradient in total ozone between the tropics and subtropics to track an expansion of the tropics in the northern hemisphere by  $\sim 1.1^\circ$  per decade over the period 1979–1991. A similar widening of the tropics was found based on the height of the thermal tropopause from radiosonde data [*Seidel and Randel*, 2007; *Reichler and Held*, 2005] and NCEP/NCAR Reanalyses [*Reichler and Held*, 2005]. The tropical expansion is also manifest in terms of tropospheric circulation and hydrology. For example, the distance between the northern and southern hemisphere subtropical jets, a measure of the width of the Hadley Cell, has grown by approximately  $2^\circ$  to  $4.5^\circ$  since 1979 based on satellite-derived tropospheric temperature gradients [*Fu et al.*, 2006]; direct estimate of the width of the Hadley cell based on meridional mass streamfunction using wind data from both ERA40 and NCEP/NCAR Reanalyses [*Hu and Fu*, 2007] yields a widening of the similar order. As a consequence, the subtropical dry zone inferred from satellite measurements of outgoing long-wave

radiation (OLR) has also expanded poleward [*Hu and Fu*, 2007].

[3] Many aspects of the tropical expansion resemble future climate projections from coupled models forced by increasing greenhouse gases [*Lu et al.*, 2007; *Seidel et al.*, 2008], although the observed widening appears to have occurred faster than that simulated by the climate models [*Johanson and Fu*, 2008]. While the observed widening has been speculated to be anthropogenic in origin, no studies (to the best of our knowledge) have unambiguously identified a precise mechanism. In this study, we make use of two sets of simulations with the GFDL atmospheric model AM2.1 to investigate the origin of the widening of the tropics. In one ensemble simulation, the model is forced by the observed global evolution of SST and sea ice over the 20th century; while in the other ensemble simulation, the estimated radiative forcing from both natural and anthropogenic sources is specified along with the observed SST and sea ice conditions. Our measure of tropical width is based on the thermal tropopause metric of *Seidel and Randel* [2007], namely the frequency of occurrence of a high-altitude tropopause characteristic of the tropics. Using this definition, we find that only under radiative forcing can the model replicate the observed tropical expansion, and that SST/sea ice boundary forcing produces a contraction of the tropics. By design, the radiative forcing includes both natural and anthropogenic components and does not allow direct attribution of the trend to anthropogenic causes. Nevertheless, our understanding of the distinctive physical signatures of the different radiative forcing agents enables us to suggest that the anthropogenic component is the dominant cause of the widening. The issue of statistical significance of the widening trend in both annual mean and seasonal mean fields is also addressed.

### 2. Data and Methods

[4] Two sets of reanalysis data for the period 1958–2000 are used in this study: daily tropopause pressure data from NCEP/NCAR [*Kistler et al.*, 2001] and daily temperatures from ERA40 [*Uppala et al.*, 2005] from which we compute daily tropopause pressure. There are warnings against using the reanalysis data prior to 1979 (the beginning of assimilation of satellite data into the reanalysis) for the study of multidecadal variability [*Randel et al.*, 2000]. Thus, extra caution has to be taken when examining trends since 1958. We find that the tropopause probability density function (PDF) metric of *Seidel and Randel* [2007], which is also used in this study (see below), is much less susceptible to the effects of changes in instrumentation and observing practices than the monthly mean tropopause height. Indeed, using this metric, we do not find any spurious jumps between 1978 and 1979 in any of the derived time series of tropical width.

<sup>1</sup>National Center for Atmospheric Research, Boulder, Colorado, USA.

<sup>2</sup>Advanced Study Program, NCAR, Boulder, Colorado, USA.

<sup>3</sup>Center for Ocean-Land-Atmosphere Studies, Calverton, Maryland, USA.

<sup>4</sup>Department of Meteorology, University of Utah, Salt Lake City, Utah, USA.

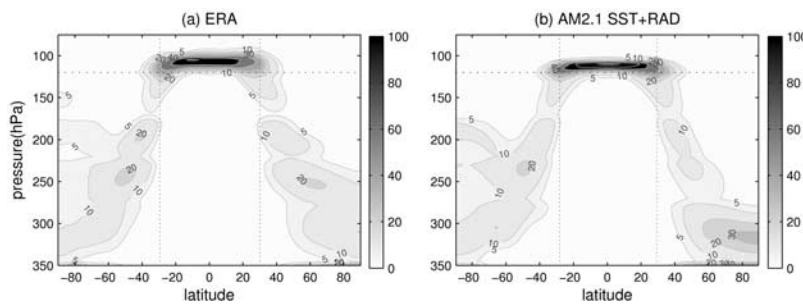


**Figure 1.** Climatological mean (1958–1999), zonally averaged annual PDF (unit is d/year) of tropopause pressure on 5-hPa bins between 75 and 350 hPa for (a) ERA40 and (b) 10 ensemble (*SST+RAD*) simulations. The two vertical lines in each panel demarcate the mean latitude of the tropical edges, which are 29.3°S and 30.0°N for ERA40 and 28.0°S and 29.2°N for the simulations.

[5] Two sets of ensemble simulations are conducted with GFDL’s atmospheric model AM2.1 (see *Delworth et al.* [2006] for model description). One set is forced by specifying the observed monthly evolution of SST and sea ice between 1870 and 2000 (referred to as *SST* experiment) and another by the SST/sea ice plus the estimated radiative forcing from both natural (solar and volcanic aerosol) and anthropogenic sources (well-mixed greenhouse gases, tropospheric and stratospheric ozone, and tropospheric aerosols) over the same period (referred to as *SST+RAD*). The radiative forcing is the same as that used for the 20th century coupled model (CM2) simulations for the Fourth Assessment Report of the Intergovernmental Panel on Climate Change (IPCC AR4 [*Hegerl et al.*, 2007]) at GFDL. It is worth noting that under the same forcing, the fully coupled GFDL CM2.1, which uses AM2.1 as its atmospheric component, can accurately replicate the globally and annually averaged lower stratospheric temperature anomalies over 1979–2003 [*Ramaswamy et al.*, 2006]. Each ensemble consists of ten members; each member starts from a different initial condition taken from previous AM2.1 simulations. Experiment *SST+RAD* simulates the past climate with the best possible knowledge of the forcing for the atmosphere, and provides the most comparable case to the real world depicted by the reanalysis data. Assuming linearity, the difference between *SST+RAD* and *SST* may be regarded as the direct response to the radiative forcing. Note that the methodology of specifying both the observed SST and radiative forcing in the atmosphere-only model does not “double count” the atmospheric radiative forcing because only the direct effect is specified and the indirect effect is included in the prescribed SST forcing, and the two effects are linearly additive in a similar experiment [*Deser and Phillips*, 2008].

[6] The daily tropopause pressure level is computed from the daily temperature data for the ERA40 reanalysis and each individual member of the AM2.1 simulations. According to the *World Meteorological Organization* [1957] definition, the tropopause level is identified as the lowest pressure level at which the lapse rate decreases to 2°C/km and the average lapse-rate between this level and all higher levels within 2 km does not exceed 2°C/km, using the algorithm of *Reichler et al.* [2003]. The NCEP/NCAR tropopause data also follows the WMO definition.

[7] For each grid point and each year/season, we computed the PDF of daily tropopause pressure by binning the

data into 5 hPa bins, from 50 hPa to 350 hPa. Figure 1 shows the climatological zonal mean of the PDFs for ERA40 and the *SST+RAD* simulations based on the period 1958–1999. The agreement between the two is encouraging, with both showing a dense concentration of low (<120 hPa, marked by the horizontal line in Figure 1) tropopause pressure values in the tropics and a bimodal distribution near the subtropics (centered at approximately 35° in each hemisphere). Following *Seidel and Randel* [2007], we associate tropopause pressures <120 hPa (or equivalently >15km) with tropical conditions and count the number of tropical tropopause days at each latitude. From this, we define the edge of the tropics as the latitude at which the number of tropical tropopause days exceeds 200 days per year. Defined this way, the mean edges of the subtropical bimodal distribution are located at the equatorward flanks of the tropics are 29.3°S (28.0°S) and 30.0°N (29.2°N) for ERA40 (AM2.1 *SST+RAD*) as indicated by the vertical dotted lines in Figure 1. The resulting annual time series of the northern and southern edges of the tropics for the period 1958–1999 (1958–2007 for NCEP/NCAR Reanalysis) are shown in Figure 2 (the starting year for our analysis is dictated by the availability of the ERA40 data set). Analogous time series for each season are provided in Figure S1 of the auxiliary material.<sup>1</sup>

[8] We estimate the linear trend between 1958 and 1999 using standard linear regression analysis. The estimated trends and their 95% confidence intervals for each season and the year as a whole are shown in Figure 3. The significance test for the trend is conducted following the method proposed by *Santer et al.* [2000]. In their proposed Student’s *t*-test, the reduction of effective degrees of freedom due to the serial correlation of the regression residuals is considered in both the estimation of the variance of the residuals and indexing of the critical *t* value. An alternative nonparametric estimate of the significance of the trend is provided in Figure S2. Both tests lead to qualitatively similar conclusions.

### 3. Results

[9] Figure 2 shows the annual time series of the tropical edges in both hemispheres for ERA40 (black) and NCEP/

<sup>1</sup>Auxiliary materials are available in the HTML. doi:10.1029/2008GL036076.

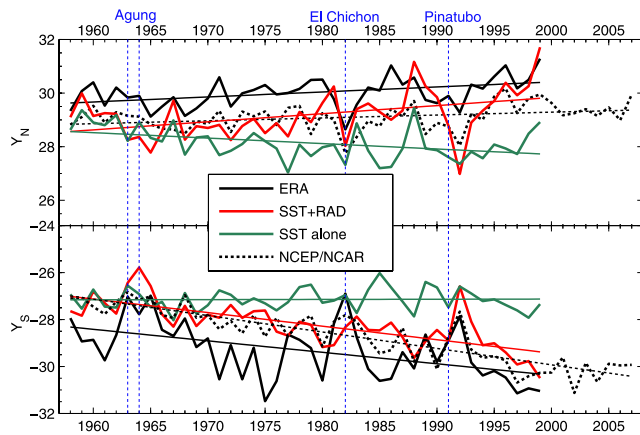


**Figure 2.** Annual time series of the location of the tropical edges, defined as the latitudes where days with tropopause pressures  $<120$  hPa (heights  $>15$  km) exceed 200 days per year. Estimates are from ERA40 (black) and NCEP/NCAR (dashed black) reanalysis data, and from the *SST* (green) and *SST+RAD* (red) simulations. The years of major volcanic eruptions are also indicated.

NCAR (dashed black) Reanalysis and the ensemble mean of *SST* (green) and *SST+RAD* (red) simulations. We stress that no large spurious discontinuity occurs between 1978 and 1979 in this PDF-based measure of tropical width for either Reanalysis. In each hemisphere, the mean latitude of the tropical edge is similar between *SST+RAD* simulation and NCEP/NCAR Reanalysis, and displaced equatorward by approximately  $1^\circ$  latitude relative to the ERA reanalysis. Thus, on average, the total width of the tropics in the NCEP/NCAR reanalysis and the ensemble mean *SST+RAD* simulation is about  $2^\circ$  latitude narrower than in the ERA40. The simulations with *SST+RAD* forcing exhibit a significant trend during 1958–1999 in each hemisphere:  $1.1^\circ$  for the northern and  $1.9^\circ$  for the southern, equivalent to  $0.71^\circ$  per decade for the total width of the tropical belt. This is similar to that estimated from the Reanalyses ( $0.70^\circ$  per decade for ERA40 and  $0.79^\circ$  per decade for NCEP/NCAR). In contrast, the simulations forced by *SST*/sea ice alone tend to produce a significant shrinking of the tropics (see Figure 3). Similar results hold for the seasonal time series (Figure 3; see also Figure S1 for the time series for each season). These findings clearly point to the critical role of direct radiative forcing in producing the widening in our measure of tropical width.

[10] Examining the seasonality of the tropical expansion, we find that both Reanalyses products exhibit significant trends in summer and fall in the northern hemisphere and in all seasons in the southern hemisphere (Figure 3). The *SST+RAD* simulation reproduces the observed seasonality reasonably well. Therefore, despite the uncertainties in the reanalyses and in the forcing of the *SST+RAD* simulation, their consensus on the significance of the tropical expansion makes a strong case for its reality. It is evident that the *SST* experiments simulate a narrowing of the tropics in all seasons in both hemispheres, with significant narrowing during winter, spring and fall in the northern hemisphere and fall in the southern hemisphere.

[11] To further demonstrate the characteristics of the tropopause trends, using DJF as an example, we plot in Figure 4 the linear trends superimposed on the climatological mean tropopause PDFs for ERA40 (Figure 4a), *SST+RAD* simulation (Figure 4b), *SST* simulation (Figure 4c), and the difference between *SST+RAD* and *SST* (Figure 4d). One striking feature in both ERA40 and *SST+RAD* is the continuous dipole structure of the trends throughout the tropics and southern hemisphere: Positive (negative) trends exist along the upper (lower) portion of the mean tropical PDFs, indicative of a rising of the mean tropopause in both the tropics and southern hemisphere extratropics (a slight upward trend is also found at high latitudes of the northern hemisphere). Decomposing the trend into *SST* forced (Figure 4c) and direct radiatively forced (Figure 4d) components, we find that both contribute to the rise of the tropical tropopause, while direct radiative forcing dominates the rise of the extratropical southern hemisphere tropopause. Even though the rise of the tropical tropopause is due to both *SST* and direct radiative forcing, the expansion of the tropical tropopause is due solely to radiative forcing as can be seen by the occurrence of positive trends at the outer periphery of the mean tropical PDF in Figure 4d.

#### 4. Summary and Discussion

[12] Simulations with GFDL's AM2.1 atmospheric general circulation model driven by the our best knowledge of forcings for the 20th century, including the observed *SST* and sea ice distributions as well as the direct radiative effects from both natural and anthropogenic sources, reproduces qualitatively, and sometimes quantitatively, the observed widening of the tropics during 1958–1999 as estimated from the ERA40 and NCEP/NCAR Reanalysis data. This result confirms the findings of *Seidel and Randel* [2007] and corroborates the reality of the expansion of the tropical belt since 1958. By contrasting the results from two sets of experiments, one forced by *SST*/sea ice alone and the other by *SST*/sea ice plus direct radiative effects, we

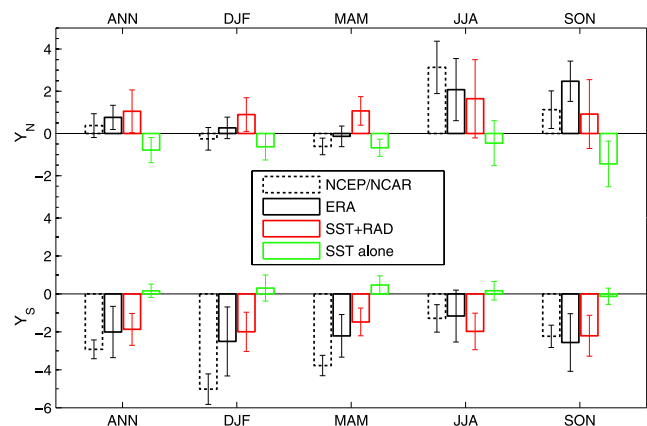


**Figure 3.** Linear trend (1958–1999) in the latitude of the tropical edge for the (top) northern and (bottom) southern hemisphere and their corresponding 95% confidence intervals (error bars). Results are based on ERA40 (solid black) and NCEP/NCAR (dashed black) reanalysis data, and on the *SST* (green) and *SST+RAD* (red) simulations.

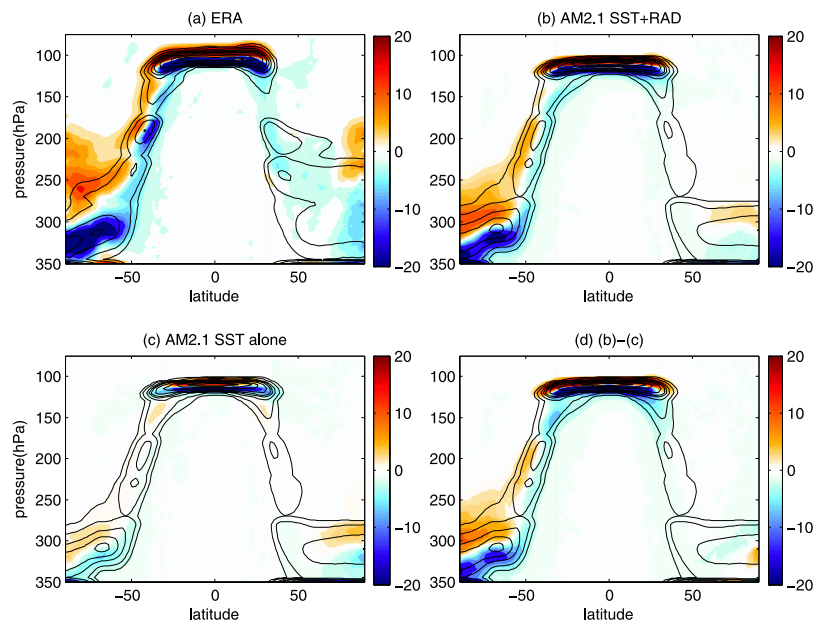


**Figure 4.** Linear trend (1958–1999) (shading) (in d/year/decade) and climatological mean (contours) of the daily tropopause pressure PDFs for DJF. Results are for (a) ERA40 reanalysis; (b) *SST+RAD*; (c) *SST*; and (d) (Figure 4b)–(Figure 4c). The two vertical lines indicate the mean latitudes of the tropical edges (33.4°S and 30.2°N for ERA40; 32.0°S and 29.5°N for the simulations).

demonstrate that our measure of tropical expansion is entirely attributable to direct radiative forcing; SST forcing alone causes no significant change in the width of the tropics, and even a contraction in some seasons. We speculate that the SST-forced contraction might result from the dominance of the upward swing of the Pacific decadal oscillation (PDO) around 1976–77 [Deser *et al.*, 2004; Zhang *et al.*, 1997] and/or the multidecadal variation in Atlantic SSTs [Delworth and Mann, 2000], for the SST pattern of the positive phase of the PDO resembles that of El Niño, which is associated with a contraction of the tropics [Lu *et al.*, 2008].

[13] Further examination of the temperature response in the model simulations (not shown) reveals that the trends in tropopause pressure and the consequent widening of the tropics is largely a result of stratospheric cooling, a feature consistent with the radiative effects of increased GHGs and stratospheric ozone depletion and in alignment with the notion that the tropopause rise over the past decades was mainly associated with stratospheric cooling but less strongly with tropospheric warming [Seidel and Randel, 2006; Austin and Reichler, 2008].

[14] In addition to well-mixed greenhouse gases and ozone, the *SST+RAD* experiment also includes variations in solar radiation, and direct scattering effects of anthropogenic and volcanic aerosols. Solar forcing has been shown to warm both the troposphere and stratosphere and should thus exert a rather weak impact on tropopause height. Both types of aerosols were shown to contribute to a downward trend in tropopause heights by warming the lower stratosphere [Santer *et al.*, 2003]. Further, we find from Figure 2 that the tropics tend to contract after major volcanic eruptions, thus providing no explanation for the widening. Taken together, the most likely culprits for the widening of the tropics since 1958 are increasing GHGs and strato-

spheric ozone depletion, both of which are of anthropogenic origin. Identification of their separate roles would require additional experiments with each radiative forcing agent considered individually.

[15] Finally, we underline that our results are based on the PDF of the tropopause to distinguish between tropics and extratropics. This is only one specific definition of tropical width, and its connection to other approaches, for example those based on tropospheric circulation or hydrological features, remains to be established. Preliminary analysis indicates that the connections between the different measures are complex and hence warrant further investigation.

[16] **Acknowledgments.** The authors thank David Schneider for reading the manuscript as NCAR internal reviewer. We are indebted to Tom Delworth and Fanrong Zhang for designing and conducting the AM2.1 model experiments. JL is supported by the UCAR/NCAR Advanced Study Program. The National Center for Atmospheric Research is sponsored by the National Science Foundation. TR is in part supported by NSF grant ATM 0532280.

## References

- Austin, J., and T. J. Reichler (2008), Long-term evolution of the cold point tropical tropopause: Simulation results and attribution analysis, *J. Geophys. Res.*, *113*, D00B10, doi:10.1029/2007JD009768.
- Delworth, T. L., and M. E. Mann (2000), Observed and simulated multidecadal variability in the Northern Hemisphere, *Clim. Dyn.*, *16*, 661–676.
- Delworth, T. L., et al. (2006), GFDL’s CM2 global coupled climate models. Part I: Formulation and simulation characteristics, *J. Clim.*, *19*, 643–674.
- Deser, C., and A. S. Phillips (2008), Atmospheric circulation trends, 1950–2000: The relative roles of sea surface temperature forcing and direct atmospheric radiative forcing, *J. Clim.*, doi:10.1175/2008JCLI2453.1, in press.
- Deser, C., A. S. Phillips, and J. W. Hurrell (2004), Pacific interdecadal climate variability: Linkages between the Tropics and North Pacific during boreal winter since 1900, *J. Clim.*, *17*, 3109–3124.
- Fu, Q., C. M. Johanson, J. M. Wallace, and T. Reichler (2006), Enhanced mid-latitude tropospheric warming in satellite measurements, *Science*, *312*, 1179.

- Hu, Y., and Q. Fu (2007), Observed poleward expansion of the Hadley circulation since 1979, *Atmos. Chem. Phys.*, *7*, 5229–5236.
- Hudson, R. D., M. F. Andrade, M. B. Follette, and A. D. Frolov (2007), The total ozone field separated into meteorological regimes—Part II: Northern Hemisphere mid-latitude total ozone trends, *Atmos. Chem. Phys.*, *6*, 5183–5191.
- Hegerl, G. C., et al. (2007), Understanding and attributing climate change, in *Climate Change 2007: The Physical Science Basis. Contribution of Working Group I to the Fourth Assessment Report of the Intergovernmental Panel on Climate Change*, edited by S. Solomon et al., pp. 663–745, Cambridge Univ. Press, Cambridge, U.K.
- Johanson, C., and M. Fu (2008), Hadley cell widening: Model simulations versus observations, *J. Clim.*, doi:10.1175/2008JCLI2620.1, in press.
- Kistler, R., et al. (2001), The NCEP/NCAR 50-year reanalysis: Monthly means CD-ROM and documentation, *Bull. Am. Meteorol. Soc.*, *82*, 247–267.
- Lu, J., G. A. Vecchi, and T. Reichler (2007), Expansion of the Hadley cell under global warming, *Geophys. Res. Lett.*, *34*, L06805, doi:10.1029/2006GL028443.
- Lu, J., G. Chen, and D. Frierson (2008), Response of the zonal mean atmospheric circulation to El Niño versus global warming, *J. Clim.*, *21*, 5835–5851.
- Ramaswamy, V., M. D. Schwarzkooph, W. J. Randel, B. D. Santer, B. J. Soden, and G. L. Stenchikov (2006), Anthropogenic and natural influence in the evolution of lower stratospheric cooling, *Science*, *311*, 1138–1141.
- Randel, W. J., F. Wu, and D. J. Gaffen (2000), Interannual variability of the tropical tropopause derived from radiosonde data and NCEP reanalyses, *J. Geophys. Res.*, *105*, 15,509–15,523.
- Reichler, T., M. Dameris, and R. Sausen (2003), Determining the tropopause height from gridded data, *Geophys. Res. Lett.*, *30*(20), 2042, doi:10.1029/2003GL018240.
- Reichler, T. J., and I. M. Held (2005), Evidence for a widening of the Hadley cell, paper presented at the 17th AMS Conference on Climate Variability and Change, Am. Meteorol. Soc., Cambridge, Mass.
- Santer, B. D., T. M. L. Wigley, J. S. Boyle, D. J. Gaffen, J. J. Hnilo, D. Nychka, D. E. Parker, and K. E. Taylor (2000), Statistical significance of trends and trend differences in layer-average atmospheric temperature time series, *J. Geophys. Res.*, *105*, 7337–7356.
- Santer, B. D., et al. (2003), Contributions of anthropogenic and natural forcing to recent tropopause height changes, *Science*, *301*, 479–483.
- Seidel, D. J., and W. J. Randel (2006), Variability and trends in the global tropopause estimated from radiosonde data, *J. Geophys. Res.*, *111*, D21101, doi:10.1029/2006JD007363.
- Seidel, D. J., and W. J. Randel (2007), Recent widening of the tropical belt: Evidence from tropopause observations, *J. Geophys. Res.*, *112*, D20113, doi:10.1029/2007JD008861.
- Seidel, D. J., Q. Fu, W. J. Randel, and T. J. Reichler (2008), Widening of the tropical belt in a changing climate, *Nat. Geosci.*, *1*, 21–24.
- Uppala, S. M., et al. (2005), The ERA40 reanalysis, *Q. J. R. Meteorol. Soc.*, *131*, 2961–3012.
- World Meteorological Organization (1957), Meteorology—A three-dimensional science: Second session of the commission for aerology, *WMO Bull.*, *4*, 134–138.
- Zhang, Y., J. M. Wallace, and D. S. Battisti (1997), ENSO-like interdecadal variability: 1900–93, *J. Clim.*, *10*, 1004–1020.

C. Deser, Climate and Global Dynamics Division, National Center for Atmospheric Research, P.O. Box 3000, Boulder, CO80307, USA.

J. Lu, Center for Ocean-Land-Atmosphere Studies, 4041 Powder Mill Road, Suite 302, Calverton, MD 20705, USA. (jianlu@cola.iges.org)

T. Reichler, Department of Meteorology, University of Utah, 135 S 1460E, Salt Lake City, UT 84112, USA.